Manescu et al. Int J Radiol Imaging Technol 2016, 2:010
Volume 2 | Issue 1

International Journal of
Radiology and Imaging Technology

Original Research: Open Access

On Long Term Effects of Low Power Laser Therapy on Bone Repair: A Demonstrative Study by Synchrotron Radiation-based Phase-Contrast Microtomography

Adrian Manescu[1#], Roxana Oancea[2#], Carmen Todea[3#], Laura Cristina Rusu[4], Serena Mazzoni[1], Meda Lavinia Negrutiu[5], Cosmin Sinescu[5] and Alessandra Giuliani[1]*

[1]Dip. di Scienze Cliniche Specialistiche e Odontostomatologiche, Università Politecnica delle Marche, 60131 Ancona, Italy

[2]Department of Preventive Community in Oral Health, Victor Babeș University of Medicine and Pharmacy Timisoara, Faculty of Dental Medicine, Str. Bulevardul Revolutiei 1989, Romania

[3]Department of Oral Rehabilitation & Dental Emergencies, Victor Babeș University of Medicine and Pharmacy Timisoara, Faculty of Dental Medicine, Str. Bulevardul Revolutiei 1989, Romania

[4]Department of Technology of Dental Materials and Devices in Dental Medicine, Victor Babeș University of Medicine and Pharmacy Timisoara, Faculty of Dental Medicine, Str. Bulevardul Revolutiei 1989, Romania

[5]Department of Propaedeutics and Dental Materials, Victor Babeș University of Medicine and Pharmacy Timisoara, Faculty of Dental Medicine, Str. Bulevardul Revolutiei 1989, Romania

[#]Authors equally contributed

***Corresponding author:** *Alessandra Giuliani, Dip. di Scienze Cliniche Specialistiche e Odontostomatologiche, Università Politecnica delle Marche, Via Brecce Bianche 1, 60131 Ancona, Italy, Tel: +390712204603, Fax: +390712204605, E-mail: a.giuliani@univpm.it*

Abstract

Laser effects on fracture healing are still controversial and require further quantitative 3D measures of newly formed bone microstructural parameters. We performed a demonstrative investigation, by synchrotron radiation-based phase-contrast microtomography (SR-phc-microCT), on bone regeneration process in rats submitted to femoral osteotomy and treated with low power laser therapy (LPLT).

Six Wistar rats were subjected to transverse osteotomy of the right and left femurs and randomly divided into four experimental groups: not grafted with biomaterials and not laser-treated (Group I, n = 3), not grafted with biomaterials but laser-treated (Group II, n = 3), grafted with biomaterials and not laser-treated (Group III, n = 3), grafted with biomaterials and laser-treated (Group IV, n = 3). LPLT was performed at dose of 16 J/cm^2 per exposure, immediately after osteotomy, every 48 hours for the first week and every 72 hours for the next two weeks. Animals were sacrificed after 24 days. Bone regeneration and mineralization degree, with or without biomaterial's grafts, were evaluated by SR-phc-microCT.

We observed that, for regenerated bone struts in the dimensional ranges thicker than 200 μm and in absence of any biomaterial graft, the bone volume percentage in the LPLT-treated samples was almost two-fold greater vs. the controls. This effect is magnified in presence of Bioss grafts when the bone volume percentage in the LPLT-treated samples was found to be almost three-fold greater vs. not treated samples.

Despite the reduced sample size, we demonstrated that SR-phc-microCT technique can play a fundamental role in the advanced characterization of laser-treated sites. In fact it allows, in a nondestructive way, a quantitative, statistically significant and high-resolution 3D analysis of newly formed bone microstructural parameters, keeping the sacrificed animals to the minimum in accordance with recent ethical standards.

Keywords

Biomaterials, Bone healing, Osteotomy, Phase contrast Microtomography, Laser therapy

Introduction

Since the first laser was realized in 1960, it has been used for surgery, diagnostics, and therapeutic medical applications [1]. Subsequently in 1980s, several studies explored bone healing after laser irradiation using several diagnostic techniques [2-5].

Several authors [6,7] demonstrated that laser irradiation at the grafted site stimulated osteogenesis during the initial stages (first 2 weeks) of the healing process and that this effect was dose dependent. It was also shown that, after 30 days of laser treatment, the healing of bone defects and the resorption of particles of the graft material was accelerated [8].

In any case the results are still controversial: while some authors

ClinMed International Library

Citation: Manescu A, Oancea R, Todea C, Rusu LC, Mazzoni S, et al. (2016) On Long Term Effects of Low Power Laser Therapy on Bone Repair: A Demonstrative Study by Synchrotron Radiation-based Phase-Contrast Microtomography. Int J Radiol Imaging Technol 2:010

Received: January 31, 2016: **Accepted:** March 28, 2016: **Published:** March 30, 2016

argued that the laser effect might accelerate fracture healing, modulating the function of osteocytes [2,9] and photo activating osteoblastic cells [3], David et al. [10] observed, by radiological and histological examinations, that osteotomy sites failed to show any enhancing effect of laser radiation on the bone healing process. They argued that their results were more reliable than previous studies because they used objective biomechanical outcome measures rather than only conventional techniques such as histology or radiology [10].

In fact at the tissue level of organization, microscopy techniques attempting to visualize the tissue-rebuilding process, such as light, fluorescence, scanning and transmission electron microscopy, are limited to two dimensional (2D) local information or otherwise require laborious three-dimensional (3D) reconstruction of serial sections. Furthermore, conventional and digital X-ray radiology are imaging methods that present several important limitations linked to their 2D nature: radiographs provide a two-dimensional image of a three-dimensional object, not accurately replicating the anatomy that is being assessed. Anatomical structures may superimpose causing anatomical or background noises, leading to difficulty in interpreting radiographs. Normally, 2D radiographs show less severe bone damages than those actually present and do not reveal the soft-tissue to hard-tissue relationships [11].

Therefore, in order to give more support and more effective therapeutic outcomes, more research is needed in this field, eventually supported by advanced 3D imaging techniques, to clarify the laser effect on bone healing process, especially in stages longer than 2 weeks.

The impact of the CT technique has been revolutionary, enabling to view internal sample details with unprecedented precision and in a non-destructive way. Furthermore it achieves contrast discrimination up to one thousand times better than conventional radiography. In this context computed microtomography (microCT) could play a major role for a complete and reliable characterization of the bone rebuilding process [12,13]. This is a powerful tool for a better understanding of the morphological characteristics of the site of interest, offering the possibility to obtain a high resolution 3D bulk reconstruction of regenerated bone in a non-destructive way. In fact several authors successfully investigated bone healing after LPLT by desktop microCT [14,15] and Cone Beam Computed Tomography (CBCT) [16]. Despite the high reliability to calculate the different morphometric parameters of the alveolar bone and the high experimental resolution in some cases [14,15], the inherent characteristics of the photons beam produced by laboratory sources often prevent reliable analysis of Bone Mineral Density (BMD) and of the bone healing process itself.

The use of X-rays delivered by Synchrotron facilities has several advantages compared to X-rays produced by laboratory sources; it includes the possibility to take advantage of the high photon flux, which guarantees the achievement of really high spatial resolutions with good signal-to-noise ratio. Furthermore, the synchrotron-produced X-ray beam is tunable: this allows performing measurements at different energies, guaranteeing an optimal evaluation of the mineralization degree in bone tissues. The use of monochromatic X-ray radiation also eliminates different artifacts, such as the beam hardening effect [17]. Synchrotron Radiation-based MicroCT was successfully applied for advanced characterization of bone [18,19], in bone tissue engineering [20-22] and other medical fields [23-25].

Furthermore, third-generation synchrotron light sources produce brilliant photon beams of spatial and temporal coherence properties at the sample stage which are suitable for routine application of phase sensitive X-ray imaging methods. Heterogeneous materials with a narrow range of attenuation coefficients (like bone during healing process) produce insufficient contrast for absorption imaging. For such materials, the imaging quality can be enhanced through the use of phase contrast tomography, obtained by performing the experiment with an increased distance between sample and detector.

In this context, the aim of this study was to explore, for the first time to the authors' knowledge, the possible use of Synchrotron Radiation-based phase-contrast MicroCT (SR-phc-microCT) to study the bone regeneration process in rats with femoral osteotomy treated with low power laser therapy (LPLT). Despite the reduced sample size due to the demonstrative purpose of this analysis, statistically supported comparisons were also assessed between spontaneous healing and healing supported by BiOss grafts (in presence or absence of LPLT) in order to show the SR-phc-microCT ability to quantitatively detect significant differences even involving a reduced number of animal models.

Materials and Methods

In this study the standards for educational and scientific practice of vivisection of animals (Law 6638 from May 8, 1979) were adopted, and the procedure was approved by the Ethics and Research Committee of Victor Babes University of Medicine and Pharmacy. All experiments underwent full protection according to the European Convention for the Protection of Vertebrate Animals used for Experimental and Other Scientific Purposes (Strasbourg, France, 1986) and to all European understandings signed by Romanian country (EU Directive 93/35/EEC, Amendment 76/768/EEC, directive 86/609 CEE), as well as the Romanian law (Law 471/2002, Ordinance 37/2002).

Six young adult (6 months old) male Wistar rats (Rattus Norvegicus), weighing around 300 g at the osteotomy stage, kept in an environment with controlled light (12 hours cycles light and dark) and controlled temperature (23°C), with animal food and water ad libitum were used. The study was developed in the vivarium of Laboratory of Victor Babes UMF. All animals underwent surgical procedure for inducing cortical bone defect (osteotomy) in right and left femur diaphysis and were sacrificed 24 days after surgery. Subsequently four groups of samples were constituted because for each animal the left leg was subjected to spontaneous regeneration while the hole of the right leg was filled with a mixture made of collagen and BiOss particles (20112 Geistlich Bio-Oss®, Geistlich Pharma North America, Princeton, NJ 08540).

Briefly, in group I (control group - Ctr; n = 3) the bone defects received no treatment; samples of group II (n = 3) were treated with LPLT but without the defect filling with the biomaterial; the group III (n = 3) was constituted of defects filled with the biomaterial but not LPLT-treated; the last group (group IV; n = 3) was finally composed of bone defects filled with the biomaterial and LPLT-treated.

Defect filler preparation

Small porous granules (20112 Geistlich Bio-Oss®) mixed to collagen bonding were used. The particles dimension in diameter varied between 500 μm and 1000 μm, with macroporosities of 100 - 400 μm and microporosities smaller than 10 μm, gradually delivering calcium and phosphate ions, attempting to support the recruitment and the colonization of osteoprogenitor cells.

Surgical procedure

After anesthesia, an incision of approximately 3 cm length in the surface of the skin and muscle were performed, separating soft tissues and periosteum, exposing the femoral region. The circular osteotomy, approximately 3 mm in diameter, was performed using Surgic XT Plus, a surgical motor which provides speed and high torque accuracy for maximum safety during operation.

Closure of the surgical site was performed with continuous suture in 2 planes of the muscles and interrupted stitches of the skin with Prolene 5/0 thread. Antibiotic prophylaxis (Cefazolin 15 mg/kg + Gentamicin 1.5 mg/kg) was administered during the surgery to guard against infection. Postoperatively all the animals receive 5 days long analgesic medication with Buprenorphine 0.05 mg/kg SC.

Laser treatment

Low power laser treatment (LPLT) was performed in groups II and IV immediately after osteotomy, every 48 hours for the first week and every 72 hours for the next two weeks. The laser equipment is represented by a Gallium - Aluminum - Arsenide laser (GaAlAs)

(IRRADIA Mid-Laser® Stockholm, Sweden), with 808 nm, 450 mW probe; 10 mm diameter spot size. The animals were irradiated transcutaneous with hand piece perpendicularly positioned in contact mode with the skin. A total laser dose per exposure of 16 J/cm^2 (frequency: 2600Hz; time/exposure: 28 s) was used for each application.

Surveillance and investigations

Follow up period of the animals consisted in daily clinical examination for 21 days, with evaluation of the general clinical status (heart rate, respiratory rate, body temperature, mucosal appearance and healing of the incision, posture and locomotion). Animals were X-Rays monitored every 2 weeks from osteotomy, for the evaluation of the healing process, of vascular reaction and of radiopaque changes.

All rats were euthanatized (Thiopental overdose) 24 days after surgery.

Microstructural analysis by X-ray SR-phc-microCT

All samples of the four groups underwent advanced microstructural characterization by synchrotron-based phase-contrast microtomography (SR-phc-microCT). MicroCT experiments were performed at the SYRMEP beam line of the ELETTRA Synchrotron Radiation Facility (Trieste, Italy). The experimental conditions were selected, according to the properties of the samples. Due to the sample composition and basing on test experiments performed on the same samples, the energy of the monochromatic beam was set to 25 keV with a sample-to-detector distance of 20 cm; the resulting voxel size was $9 \times 9 \times 9$ μm^3. A total of 1200 radiographic images were recorded for each sample.

In this current study, a phase-contrast set-up was chosen. It differs from conventional X-ray imaging because the resulting images are not based solely on attenuation contrast. The effect of an X-ray beam going through the sample is described by the refractive index, $n(r) = 1 - \delta(r) + i\beta(r)$, where δ is the refractive index decrement and β is the attenuation index. As δ is much larger than the imaginary part β, the phase approach provides greater sensitivity than the absorption approach. δ is actually proportional to the mean electron density, which in turn is nearly proportional to the mass density.

The method used for quantitative volumetric reconstructions of the refractive index is based on a two-step approach: first, the phase projections are determined in the form of Radon projections (phase retrieval) and then the object function, i.e. the refractive index decrement δ, is reconstructed by applying a conventional filtered back projection (FBP) algorithm.

Typically the phase retrieval implies the reconstruction of two different real-valued 3D distributions, $\delta(r)$ and $\beta(r)$; such reconstruction generally requires acquisition of at least two different 2D projections at each view angle. However, in some cases, it can be shown *a priori* that the distributions of the real and imaginary parts of the refractive index are proportional to each other, i.e., $\beta(r) = \varepsilon\delta(r)$, where the proportionality constant ε does not depend on the spatial coordinates. This assumption is possible only for special classes of objects, such as *pure-phase* (i.e. very weakly absorbing) objects, or *homogeneous* objects, such as objects consisting predominantly of a single material (possibly, with a spatially varying density) [26]. This last case is represented by our samples where a slow variation of the complex amplitude can be assumed, considering the different bone stages (native bone, bone under remodeling, newly formed bone) present in the investigated region ("monomorphous" specimen). In this situation, a single projection per each view angle is sufficient for reconstruction of the 3D distribution of the complex refractive index [27].

In this study, a phase-retrieval algorithm based on the Transport of Intensity equation (TIE) [26,28] was applied to the acquired datasets with parameters tuned to edge enhancement reduction and balance noise minimization. A value of 200 was considered for the δ/β ratio, indicated for the bone phase in the X-TRACT software manual (CSIRO Mathematical and Information Sciences, Canberra, Australia). Then, the common filtered back-projection algorithm was used to reconstruct the slices. The X-TRACT software was applied for both the TIE-based phase retrieval and the reconstruction of X-ray phase-contrast slices.

Then, the slices stack was analyzed by using the software VG Studio MAX 1.2 (Volume Graphics, Heidelberg, Germany). Quantitative parameters were calculated directly from 3D images to characterize the full set of samples. This quantification first required segmenting the different phases to separate them from the background; a 3D median smoothing filter (kernel width = 3) was applied in order to facilitate segmentation. In the samples not grafted with the biomaterial (Groups I and II), such segmentation was easily performed by simple thresholding because the gray level histogram was clearly bimodal with a first peak corresponding to background (air) and a second peak corresponding to bone; in the Groups III and IV, however, a third peak related to the grafted BiOss appeared. The thresholds of segmentation of the gray levels distribution (0-65535; unsigned 16-bit range) were selected according to the Mixture Modeling algorithm (NIH Image J Plugin); threshold values were manually set to 34000 (bone) and 46480 (BiOss).

Representative volumes of interest (VOIs) of around $1 \times 1 \times 1$ mm^3, fully included in the bone defect, were chosen. The obtained VOIs were then analyzed in order to measure struts thickness distribution using a module of VG Studio MAX 1.2, namely the "Wall thickness analysis" module [29]. The same method was applied to extract the color maps related to the thickness distribution.

Statistical analysis

Statistical analyses were performed with SigmaStat 3.5 software (Systat Software, San Jose, California). Results are expressed as mean plus or minus standard deviation. T-test among experimental groups was used. P values ≤ 0.05 were considered statistically significant.

Results

The amount of the newly formed bone was calculated by counting the corresponding voxels underlying the peak associated with the relevant phase. The bone thickness distribution vs. the specific volume normalized to the total bone volume was assessed in the dimensional range between 20-500 μm of thickness.

The first analysis was referred to a comparison at 24 days from osteotomy between control femurs (Group I) and femurs treated by LPLT stimulation (Group II) in absence of any biomaterial. Histograms of the distribution of the bone thickness in the investigated samples are reported in figure 1A. Mean values and Standard Deviations are reported for each range of dimensional size. No significant difference has been detected for all the dimensional ranges ($p > 0.05$). The color maps of the newly-formed bone thickness distribution seem to confirm that no significant differences exist in newly formed bone thickness distribution between controls (Figure 1B) and LPLT-treated samples (Figure 1C). Even if this is in agreement with some literature [10], at a closer reading of the histogram trend in figure 1A it is clear that while for control femurs only ~17% of the bone volume is in the size range thicker than 200 μm, femurs LPLT-stimulated presented more than 29% of the bone volume in the same range, indicating the presence of thicker struts in the treated samples.

In order to validate previous results referred to the effects of low-power laser irradiation on the repair of bone defects, we also compared at 24 days from osteotomy control femurs (Group III) and femurs treated by LPLT stimulation (Group IV) when the defect had been filled with a mixture including BiOss particles. Histograms of the distribution of the bone thickness in the investigated samples are reported in figure 2A. Mean values and Standard Deviations are reported for each range of dimensional size. Even in this case no significant difference has been detected for all the dimensional ranges ($p > 0.05$) and the color maps of the newly-formed bone thickness

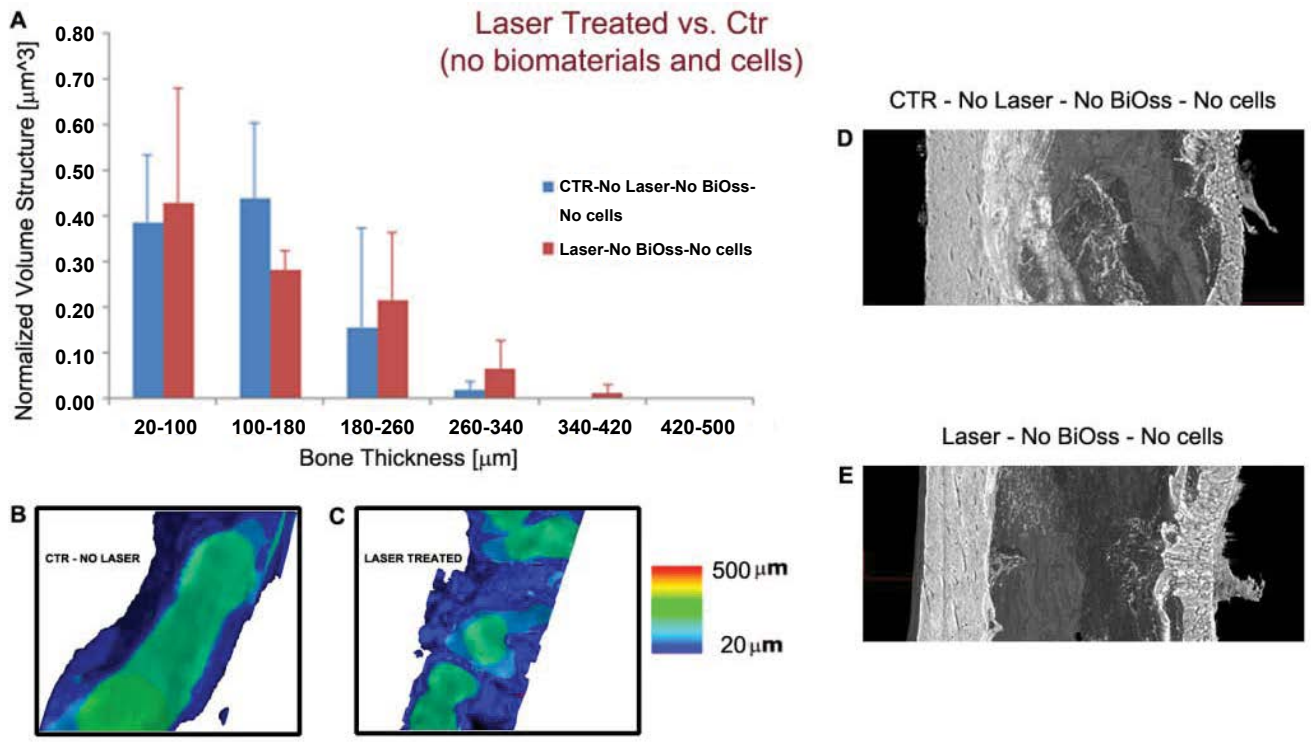

Figure 1: Laser-treated (Group II) vs. Ctr (Group I), without biomaterial or cells grafts. (**A**) Quantification of newly formed bone thickness distribution. The values reported are the average of the three samples per group. No significant difference has been detected for all the dimensional ranges. On the other hand the histogram trend clearly shows that while for control femurs only ~17% of the bone volume is in the size range thicker than 200 µm, femurs LPLT-stimulated presented more than 29% of the bone volume in the same range, indicating the presence of thicker struts in the treated samples; (**B-C**) Color map of bone thickness distribution in Ctr (B) and in a Laser-treated sample (C); (**D-E**) Longitudinal section of the 3D reconstruction of portions of treated femurs. Left wall: healthy native bone; right wall: portion submitted to osteotomy in a Ctr (D) and a laser-treated (E) sample. Both control femurs and femurs treated by LPLT stimulation presented a regenerated bone with cortical structure reproducing the native bone of the left wall.

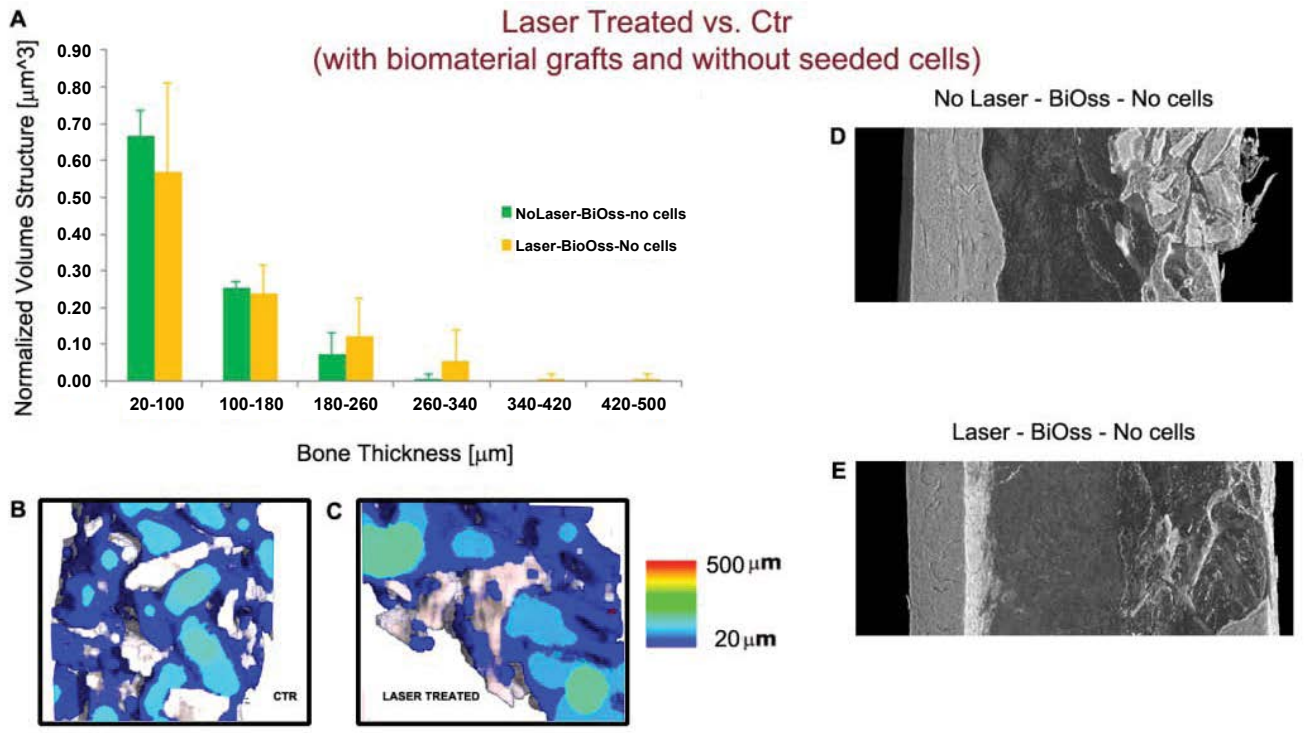

Figure 2: Laser-treated (Group IV) vs. Ctr (Group III), with biomaterial (BiOss) grafts. (**A**) Quantification of newly formed bone thickness distribution. The values reported are the average of the three samples per group; (**B-C**) Color maps of bone thickness distribution in Ctr (B) and Laser-treated samples (C); No significant difference has been detected for all the dimensional ranges. On the other hand the histogram trend clearly shows that while for not LPLT-treated femurs only ~8% of the bone volume is in the size range thicker than 200 µm, femurs LPLT-stimulated presented more than 21% of the bone volume in the same range, indicating the presence of thicker struts in the treated samples; (**D-E**) Longitudinal section of the 3D reconstruction of portions of treated femurs. Left wall: healthy native bone; right wall: portion submitted to osteotomy and biomaterial graft in a Ctr (D) and a laser-treated (E) sample. Both control femurs and femurs treated by LPLT stimulation still did not show the typical morphology of the cortical structure of the native bone.

distribution (Figure 2B and Figure 2C) confirmed such result. Interestingly, also in presence of BiOss grafts, the trend in figure 2A indicates that not LPLT-treated femurs have ~8% of the bone volume in the size range thicker than 200 µm, against the 21% for the LPLT-

treated samples, confirming the presence of thicker struts in the LPLT-treated samples.

Moreover the results described in figure 2 revealed interesting information if correlated to the observation of the bone regeneration, at 24 days from osteotomy, in absence (Group I) or presence (Group III) of the biomaterial graft and without any laser treatment. These data are shown in figure 3; in presence of the BiOss grafts, the newly formed bone struts, in the range of 20-120 μm, are significantly more present ($p = 0.041$) than in control samples (Figure 3A, Figure 3B and Figure 3C) . This gap is reduced ($p > 0.05$) in the case of samples LPLT-treated (Group II vs. Group IV: data not shown), confirming the positive effect of the LPLT treatment in favoring bone repair in presence of the biomaterial.

The information was confirmed by the longitudinal sections of the 3D reconstructions (Figure 1D, Figure 1E, Figure 2D and Figure 2E). The left wall of each femur is the native bone, while the right wall is the portion submitted to osteotomy, 24 days after the surgical procedure. In the case of the samples not grafted with the BiOss, both control femurs (Group I, Figure 1D) and femurs treated by LPLT stimulation (Group II, Figure 1E) presented a regenerated bone with cortical structure reproducing the native bone of the left wall (lamellae, Harvesian system, etc.). Mean thickness of the regenerated bone in the LPLT-treated femur was higher than the regenerated bone in control samples; interestingly, by observation of the morphological structure, the newly formed bone in LPLT-treated samples show peripheral portions similar to trabecular struts. Differently, in the case of the samples grafted with the BiOss, both control femurs (Group III, Figure 2D) and femurs treated by LPLT stimulation (Group IV, Figure 2E) still did not show the typical morphology of the cortical structure of the native bone. Mean thickness of the newly formed bone is comparable in absence or presence of laser stimulation but is significantly lower than in absence of BiOss grafts, confirming the results shown in figure 3.

We studied also the mineralization degree ρ [mgHA/cm^3] of the newly formed bone, comparing this with the native bone, 24 days from osteotomy and from the beginning of laser treatment. While we found no significant differences ($p > 0.05$) in mineralization of the regenerated bone in presence or absence of laser treatment, the bone mineralization of the regenerated sites was significantly ($p < 0.001$) lower than in healthy native sites, independently from laser treatment.

Discussion

Most scientific studies agree to observe the beneficial effects of LPLT in bone formation in the early stages (first 2 weeks) of the healing process. On the other hand some studies [10,30-32] cast doubt on such effects in the consolidation period of distraction osteogenesis and in later stages. Because of that we fixed our time-point of analysis at 24 days from osteotomy, i.e. during the consolidation time.

At this time-point it was observed that the defects which underwent treatment with laser did not present an overall significant difference in newly formed bone thickness distribution respect to controls. This was shown true also in presence of BiOss grafts. This thickness distribution analysis, that seems in agreement with some results presented in the literature [10] (especially for long term stages [30-32]), by reason of the peculiar characteristics of the analysis carried out with a monochromatic X-Ray beam and phase contrast set-up, lends itself to a second reading and a more in-depth interpretation which takes into account the bone volume percentage in each dimensional range. It turns out that, for dimensional ranges thicker than 200 μm and in absence of any biomaterial graft, the bone volume percentage in the LPLT-treated samples was almost two-fold greater vs. the same parameter in controls. This effect is magnified in presence of BiOss grafts when the bone volume percentage in the LPLT-treated samples was found to be almost three-fold greater vs. not treated samples.

The accuracy of our newly formed bone thickness distribution analysis was also confirmed by the fact that in presence of the BiOss grafts and without any laser treatment, the newly formed bone struts, in the range of 20-120 μm, are significantly more than in control samples. This seems due to the osteoinduction and osteoconduction processes accelerated by the presence of the biomaterial filling the defect. In fact BiOss was demonstrated to develop newly-formed bone, partly invaginating the particles of apatite and forming bridges in the form of trabeculae between the individual BiOss particles [33]. Interestingly these differences were reduced with laser administration; in fact as previously shown in figure 1A and figure 2A, the laser treatment seems to accelerate the osteoinduction and osteoconduction processes in presence of biomaterial grafts [34,35].

From a morphological point of view we observed that, in the case of the samples grafted with the BiOss, both control femurs and femurs treated by LPLT stimulation delay in showing the typical cortical morphology. This can be explained considering that the shape, the morphology and the structure of the BiOss particles mismatch with the native bone characteristics, requiring longer times for adhesion, cells colonization and bone healing.

In terms of mineralization [mgHA/cm^3] of the regenerated bone, we found no significant differences in presence or absence of laser treatment: this result was strongly expected because our study was performed 24 days after osteotomy and other authors observed that the positive effect of laser therapy in bone mineralization is time-dependent and that no differences with controls are observed after 21 days [36].

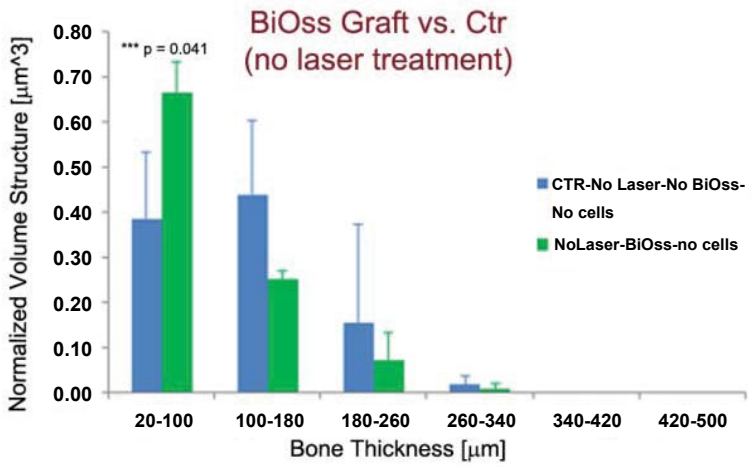

Figure 3: BiOss grafted (Group III) vs. Ctr (Group I), without laser treatment. Quantification of newly formed bone thickness distribution. In presence of the BiOss grafts, the newly formed bone struts, in the range of 20-120 μm, are significantly more present than in control samples. The values reported are the average of the three samples per group. ***$p < 0.05$ - Significant mismatch in thickness.

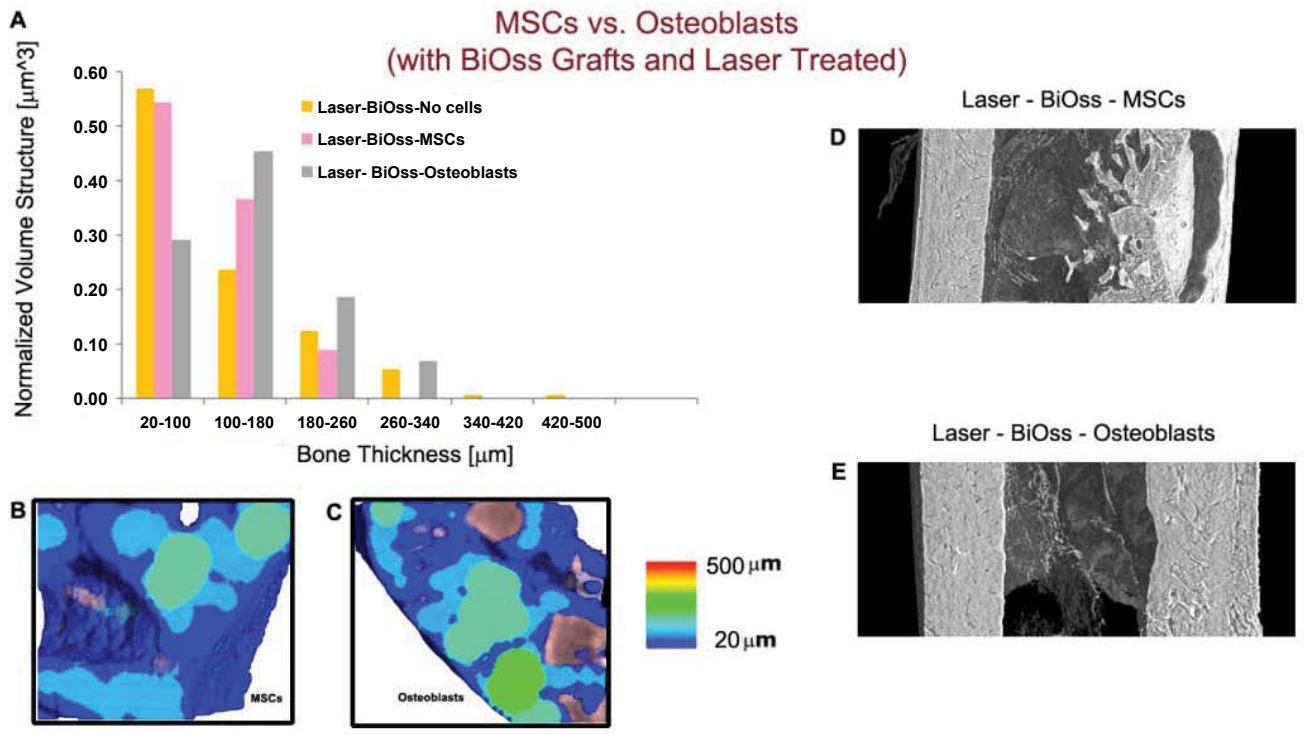

Figure 4: MSCs vs. Osteoblasts culture in a defect filler, with biomaterial and laser treatment. (**A**) Quantification of newly formed bone thickness distribution; (**B-C**) Color map of bone thickness distribution in presence of a MSCs culture (B) and of a Osteoblasts culture (C); (**D-E**) Longitudinal section of the 3D reconstruction of portions of treated femurs. Left wall: healthy native bone; right wall: portion submitted to osteotomy. The bone defect filler including the osteoblasts culture seems to be the condition morphologically and morphometrically closer to the healthy native bone of the investigated bone site.

For the sake of completeness, we also carried out few tests on samples in which, in addition to laser treatment and the use of BiOss as filler, a culture of mesenchymal stem cells (MSCs) or of osteoblasts was added to the mixture graft (Figure 4).

From the histogram (Figure 4A), from the color maps (Figure 4B and Figure 4C) and from the 3D reconstructions of the treated sites (Figure 4D and figure 4E), it was clear that the bone defect filler including the osteoblasts culture seems to be the condition morphologically and morphometrically closer to the healthy native bone of the investigated bone site. Several studies seem to confirm this experimental evidence [37,38].

However, despite the reduced number of samples due to its demonstrative nature, this work undoubtedly proves that SR-phc-microCT studies looking at bone healing over time (in presence or absence of any laser treatment), play a fundamental role in the advanced characterization of treated sites because it allows, in a nondestructive way, a quantitative, statistically significant and high-resolution 3D analysis of newly formed bone microstructural parameters, keeping the sacrificed animals to the minimum in accordance with recent ethical standards.

Acknowledgements

ELETTRA User Office is kindly acknowledged for providing beam time for the microCT experiments. We deeply thank Dr. Giuliana Tromba for her help at SYRMEP beamline. The work derived from collaboration activities within the framework of the MPNS Action COST MP1005 “From nano to macro biomaterials (design, processing, characterization, modeling) and applications to stem cells regenerative orthopedic and dental medicine (NAMABIO)”. The research activity was partially funded by Romanian Authority for Scientific Research under Partnership (grant CNDI–UEFISCDI, PN-II-PT-PCCA-2011-3.2-1682 (http://3om-group-optomechatronics.ro/)) and Victor Babes University of Medicine and Pharmacy Timisoara, Romania (Project no. PIII-C2-PCFI (2015-2016), DENTALOCT).

Ethical Standards

The animal studies have been approved by the appropriate ethics committee and have therefore been performed in accordance with the ethical standards laid down in the 1964 Declaration of Helsinki and its later amendments.

References

1. Brighton CT, Hunt RM (1997) Early histologic and ultrastructural changes in microvessels of periosteal callus. J Orthop Trauma 11: 244-253.
2. Trelles MA, Mayayo E (1987) Bone fracture consolidates faster with low-power laser. Lasers Surg Med 7: 36-45.
3. Yamada K (1991) Biological effects of low power laser irradiation on clonal osteoblastic cells (MC3T3-E1). Nihon Seikeigeka Gakkai Zasshi 65: 787-799.
4. Tang XM, Chai BP (1986) Effect of CO2 laser irradiation on experimental fracture healing: A transmission electron microscopic study. Lasers Surg Med 6(3):346-352.
5. Motomura K, Nakajima M, Ihara A, Atsumi K (1984) Effects of various laser irradiation on callus formation after osteotomy. Nippon Reza Igakkai Shi. The Journal of Japan Society for Laser Medicine 4:195-196.
6. da Silva RV, Camilli JA (2006) Repair of bone defects treated with autogenous bone graft and low-power laser. J Craniofac Surg 17: 297-301.
7. Weber JB, Pinheiro AL, de Oliveira MG, Oliveira FA, Ramalho LM (2006) Laser therapy improves healing of bone defects submitted to autologous bone graft. Photomed Laser Surg 24: 38-44.
8. Cunha MJS, Esper LA, Sbrana MC, de Oliveira PGFP, do Valle AL, et al. (2014) Effect of Low-Level Laser on Bone Defects Treated with Bovine or Autogenous Bone Grafts: In Vivo Study in Rat Calvaria. BioMed Research International 2014.
9. Khadra M (2005) The effect of low level laser irradiation on implant-tissue interaction. In vivo and in vitro studies. Swed Dent J Suppl : 1-63.
10. David R, Nissan M, Cohen I, Soudry M (1996) Effect of low-power He-Ne laser on fracture healing in rats. Lasers Surg Med 19: 458-464.
11. Shah N, Bansal N, Logani A (2014) Recent advances in imaging technologies in dentistry. World J Radiol 6: 794-807.
12. Claesson T (2001) A medical imaging demonstrator of computed tomography and bone mineral densitometry. Stockholm: Universitetsservice US AB, Stockholm.
13. Cancedda R, Cedola A, Giuliani A, Komlev V, Lagomarsino S, et al. (2007) Bulk and interface investigations of scaffolds and tissue-engineered bones by X-ray microtomography and X-ray microdiffraction. Biomaterials 28: 2505-2524.

14. Romão MM , Marques MM, Cortes AR, Horliana AC, Moreira MS, et al. (2015) Micro-computed tomography and histomorphometric analysis of human alveolar bone repair induced by laser phototherapy: a pilot study. International Journal of Oral and Maxillofacial Surgery 44: 1521-1528.

15. Kim SJ, Moon SU, Kang SG, Park YG (2009) Effects of low-level laser therapy after Corticision on tooth movement and paradental remodeling. Lasers Surg Med 41: 524-533.

16. Cenci R, Silveira V, Mayer L, Oliveira H, Moraes J, et al. (2015) Analysis by means of cone-beam computed tomography, bone density and X-ray beam attenuation of rabbit mandibles subjected to low-level laser therapy during distraction osteogenesis. Rev. Ciênc Méd Biol 14: 30-35.

17. Giuliani A, Komlev V, Rustichelli F (2010) Three-Dimensional Imaging by Microtomography of X-ray Synchrotron Radiation and Neutrons. In: Skrzypek JJ, Rustichelli F, Innovative Technological Materials. Springer Berlin Heidelberg: 123-177.

18. Canciani B, Ruggiu A, Giuliani A, Panetta D, Marozzi K, et al. (2015) Effects of long time exposure to simulated micro- and hypergravity on skeletal architecture. J Mech Behav Biomed Mater 51: 1-12.

19. Tavella S, Ruggiu A, Giuliani A, Brun F, Canciani B, et al. (2012) Bone turnover in wild type and pleiotrophin-transgenic mice housed for three months in the International Space Station (ISS). PLoS One 7: e33179.

20. Manescu A, Giuliani A, Mohammadi S, Tromba G, Mazzoni S, et al. (2016) Osteogenic potential of dualblocks cultured with human periodontal ligament stem cells: in vitro and synchrotron microtomography study. J Periodontal Res 51: 112-124.

21. Giuliani A, Manescu A, Larsson E, Tromba G, Luongo G, et al. (2014) In vivo regenerative properties of coralline-derived (biocoral) scaffold grafts in human maxillary defects: demonstrative and comparative study with Beta-tricalcium phosphate and biphasic calcium phosphate by synchrotron radiation x-ray microtomography. Clin Implant Dent Relat Res 16: 736-750.

22. Giuliani A, Manescu A, Langer M, Rustichelli F, Desiderio V, Paino F, De Rosa A, Laino L, D'Aquino R, Tirino V, Papaccio G. (2013) Three years after transplants in human mandibles, histological and in-line HT revealed that stem cells regenerated a compact rather than a spongy bone: biological and clinical implications. Stem Cells Transl Med 2: 316-324.

23. Giuliani A, Frati C, Rossini A, Komlev VS, Lagrasta C, et al. (2011) High-resolution X-ray microtomography for three-dimensional imaging of cardiac progenitor cell homing in infarcted rat hearts. J Tissue Eng Regen Med 5: e168-178.

24. Farini A, Villa C, Manescu A, Fiori F, Giuliani A, et al. (2012) Novel insight into stem cell trafficking in dystrophic muscles. Int J Nanomedicine 7: 3059-3067.

25. Rominu M, Manescu A, Sinescu C, Negrutiu ML, Topala F, et al. (2014) Zirconia enriched dental adhesive: A solution for OCT contrast enhancement. Demonstrative study by synchrotron radiation microtomography. Dent Mater 30: 417-423.

26. Gureyev TE, Pogany A, Paganin DM, Wilkins SW (2004) Linear algorithms for phase retrieval in the Fresnel region. Opt Commun 231: 53-70.

27. Gureyev TE, Paganin DM, Myers GR, Nesterets YI, Wilkins SW (2006) Phase-and-amplitude computer tomography. Appl Phys Lett 89: 034102.

28. Gureyev TE, Mayo SC, Myers DE, Nesterets YA, Paganin DM, et al. (2009) Refracting Rontgen's rays: propagation based x-ray phase contrast for biomedical imaging. J Appl Phys 105:102005.

29. http://www.volumegraphics.com/en/products/vgstudio-max/wall-thickness-analysis/.

30. Farzad F, Mahdi G, Reza F, Katayoun AM, Dehghan KS, et al. (2014) Cellular Effect of Low-Level Laser Therapy on the Rate and Quality of Bone Formation in Mandibular Distraction Osteogenesis. Photomedicine and Laser Surgery 32: 315-332.

31. Peccin MS, Oliveira F, Muniz Renno AC, Pacheco de Jesus, Pozzi R, et al. (2013) Helium- neon laser improves bone repair in rabbits: comparison at two anatomic sites. Lasers in Medical Science 28: 1125-1130.

32. Ana Claudia Muniz Renno, Fernanda Mendes de Moura, NádiaSlemer Andrade dos Santos, Renata PassarelliTirico, Paulo SérgioBossini, et al. (2006) The effects of infrared-830 nm laser on exercised osteopenic rats. Lasers in Medical Science 21: 202-207.

33. Yildirim M, Spiekermann H, Biesterfeld S, Edelhoff D (2000) Maxillary sinus augmentation using xenogenic bone substitute material Bio-Oss in combination with venous blood. A histologic and histomorphometric study in humans. Clin Oral Implants Res 11: 217-229.

34. Obradovic RR, Kesic LG, Pesevska S (2009) Influence of low-level laser therapy on biomaterial osseointegration: a mini-review. Lasers Med Sci 24: 447-451.

35. Lirani-Galvao AP, Jorgetti V, Lopes da Silva O (2006) Comparative study of how low-level laser therapy and low-intensity pulsed ultrasound affect bone repair in rats. Photomed Laser Surg 24: 735-740.

36. Barbosa D, de Souza RA, Xavier M, da Silva FF, Arisawa EA, et al. (2013) Effects of low-level laser therapy (LLLT) on bone repair in rats: optical densitometry analysis. Lasers Med Sci 28: 651-656.

37. Grassi FR, Ciccolella F, D'Apolito G, Papa F, Iuso A, et al. (2011) Effect of low-level laser irradiation on osteoblast proliferation and bone formation. J Biol Regul Homeost Agents 25: 603-614.

38. Petri AD, Teixeira LN, Crippa GE, Beloti MM, de Oliveira PT, et al. (2010) Effects of low-level laser therapy on human osteoblastic cells grown on titanium. Braz Dent J 21: 491-498.